Attenuation of Ultrasonic Waves: Influence of Microstructure and Solid Fat Content

Silvana Martini[a], Constantin Bertoli[b], Maria Lidia Herrera[c], Ian Neeson[d], and Alejandro Marangoni[a,*]

[a]Department of Food Science, University of Guelph, Guelph, Ontario, Canada, [b]Nestlé Research Centre, Lausanne, Switzerland, [c]Departamento de Industrias, Facultad de Ciencias Exactas y Naturales, University of Buenes Aires, Argentina, and [d]VN Instruments Ltd., Elizabethtown, Ontario, Canada

ABSTRACT: Ultrasonic technology can be used to monitor the crystallization of fats and determine solid fat content (SFC) online. Ultrasonic waves are attenuated as crystals form and grow, and this attenuation occurs first at higher frequencies. The attenuation of the ultrasonic signal does not depend on the induction times of crystallization of the systems, or on their thermal behavior; but it does depend on SFC and on microstructure, particularly on the crystal size. At low SFC values (~5%), bigger crystals generate more attenuation. At intermediate SFC values (~10%), crystal size does not affect signal attenuation and SFC is the key factor responsible for signal attenuation. At high SFC values (up to 20%), crystal size again seems to be the factor that controls attenuation.

Paper no. J10959 in *JAOCS 82*, 319–328 (May 2005).

KEY WORDS: Attenuation, chirp, microstructure, solid fat content, synthetic impulse, ultrasonic technology.

As an ultrasonic wave travels through a material, it is attenuated, i.e., its amplitude decreases with the distance traveled. The major causes for attenuation are absorption and scattering. Absorption occurs to some extent in all materials as a result of thermodynamic relaxation mechanisms that convert energy from the ultrasonic wave into some other form, ultimately heat. Scattering is often the predominant form of attenuation in heterogeneous materials. It occurs when some of the ultrasonic waves incident upon a discontinuity in a material (e.g., a particle) are scattered in a direction that is different from that of the incident wave. Scattering can also occur owing to the formation of new interfaces in the system. Scattering of ultrasound is important in many systems since it can have a significant effect on the measured ultrasonic properties, making the velocity and attenuation dependent on particle size as well as concentration (1,2). To extract information about the physicochemical properties of many liquid materials from ultrasonic measurements, it is necessary to measure the frequency dependence of their ultrasonic properties. For example, McClements *et al*. (3) studied the frequency dependence of ultrasonic properties by analyzing emulsions with different particle sizes to obtain information about the size and concentration of scatterers in emulsions and suspensions (4).

Several studies have been published regarding the use of ultrasonic technology in food research (5–15). The major difficulty found in some of these studies was the attenuation of the ultrasonic wave in concentrated samples. Therefore, the objective of this study was to study the factors that influence the attenuation of ultrasonic waves in fat systems, in particular to establish a relationship between the attenuation, microstructure, and solid fat content (SFC) of fats during their isothermal crystallization and to analyze their dependence on the ultrasonic frequencies used. This study will help us understand the factors that somehow limit the application of ultrasonics in food analysis.

MATERIALS AND METHODS

Crystallization procedure. Five fat samples (samples 1, 2, 3, 4, and 5 with m.p. of 46.1, 43.5, 40.7, 41.2, and 36.6°C, respectively) were crystallized at 20, 25, and 30°C in a crystallization cell especially designed to monitor fat crystallization on-line by means of ultrasonic technology. Crystallization was performed under agitation using 400 rpm of shear. The cell temperature was controlled by means of water circulated from a water bath set at the particular crystallization temperature. Samples were heated to 120°C in an oven, held at this temperature for 30 min, and then introduced into the cell. The temperature profile was monitored by means of a thermocouple dipped into the sample and the crystallization process was followed by means of ultrasonics and pulsed NMR (p-NMR) for 90 min.

Ultrasonic measurements. As described by Martini *et al.* (5), ultrasonic measurements were performed by means of an SIA-7 ultrasonic spectrometer (VN Instruments Ltd., Elizabethtown, Ontario, Canada). Transducers of 550 kHz and 1 MHz center frequency (GE Panametrics, Waltham, MA) were used to generate the ultrasonic wave. A chirp pulse was used in these experiments instead of the traditional pulser signal. The chirp pulse was generated over a range of frequencies with different amplitudes. The center frequency of the chirp corresponds to the transducer center frequency (550 kHz and 1 MHz), and the range of frequencies in which these transducers operate is called the bandwidth. A synthetic impulse (SI) was

*To whom correspondence should be addressed at Department of Food Science, University of Guelph, Guelph, ON, Canada, N1G 2W1.
E-mail: amarango@uoguelph.ca

The third author is an associate researcher of the National Research Council of Argentina (CONICET).

generated from the chirp by means of a digital receiver processor. Three parameters can be measured from the SI image: integrated response (IR: area under the curve), time of flight (TF: position of the peak), and full width half maximum (FWHM: width of the peak).

SFC. SFC was measured by means of p-NMR (Bruker Optics Ltd., Milton, Ontario, Canada) as crystallization took place. Samples were taken from the crystallization cell with a Pasteur pipette and put into an NMR tube to perform the measurement. The crystallization process was followed by taking samples every minute for the first 10 min and then every 5 min until the end of crystallization process (90 min). Data reported are averages of two individual measurements. The error in the SFC determinations was 1% approximately (5).

Laser turbidimeter. The crystallization process was followed by means of a laser turbidimeter. The laser light source (He-Ne Class II laser, wavelength 633 nm, model OEM4P; Aerotech) was placed under the crystallization cell, which had a glass window in the bottom that enabled the light to pass through the sample. Once the light passed through the sample, it reached the detector, which was placed on top of the cell and which was aligned to the laser. The laser signal was then collected and processed by a computer program (HP VEE Lab., Version 5.02, 1999 Hewlett-Packard Co., 1991–1999). As crystallization occurred, the laser beam was diffracted by the fat crystals, and a deviation in the laser signal was observed. The first deviation of the signal from the baseline was used to calculate the induction times of crystallization.

Microscopy. The morphology of the crystals obtained during the crystallization process was studied by means of polarized light microscopy. An Olympus microscope (Olympus Optical Co. Ltd., Tokyo, Japan) with a digital camera attached (Model XC-75; Sony, Japan) was used to photograph the crystals. As crystallization took place, a drop of the crystallized fat was taken and placed between a slide and cover slide thermostated at the crystallization temperature. Samples were taken at different times after crystallization started and pictures were taken using 40× magnification until the end of the crystallization (90 min).

DSC. The thermal behavior of the five samples was studied using a differential scanning calorimeter (model 2910; TA Instruments, Mississauga, Ontario, Canada). After 90 min in the crystallization cell, 5–10 mg of the samples crystallized at the different crystallization temperatures was placed in sealed aluminum pans to carry out DSC. Calibration was made with indium at 5°C/min. Samples were run from crystallization temperature to 80°C at 5°C/min.

RESULTS AND DISCUSSION

Induction times of crystallization. Table 1 shows the induction times of the five samples crystallized at 20, 25, and 30°C calculated by means of laser turbidimetry and ultrasonics. As shown in this table, induction times determined by the laser turbidimeter increased as the crystallization temperature increased for all the samples, an expected result since lower crystallization temperatures cause higher supercooling in the system and result in faster crystallization (shorter induction time). At 20°C, all samples showed similar inductions times (very short) since the supercooling was very high, and therefore the crystallization was very fast. An exception to this behavior was found in sample 5 (induction time of 11.71 ± 1.0 min), which has a much lower m.p. than the other samples (36.6 vs. 46.1, 43.5, 40.7, and 41.2°C for samples 1, 2, 3, and 4, respectively). Thus, sample 5 was less supercooled and needed more time to crystallize. For 25 and 30°C, the induction times between samples varied in accordance with their m.p. Samples 3 and 4 had similar m.p., and thus their inductions times were not significantly different at 20 and 25°C, but sample 4 showed a significantly higher induction time than sample 3 when crystallized at 30°C. This suggests that although these samples have similar m.p., their crystallization behavior at different temperatures is different.

TABLE 1
Induction Times[a] (τ, min) of Crystallization Determined by Laser Turbidimetry and Ultrasonics for Fat Samples Crystallized at 20, 25, and 30°C

	Laser turbidimetry			Integrated response (IR)		
Sample	20°C	25°C	30°C	20°C	25°C	30°C
1	1.0 ± 0.3	1.7 ± 0.9	2.5 ± 0.5	7.2 ± 0.4	6.8 ± 2.2	9.1 ± 1.8
2	2.0 ± 0.2	3.6 ± 0.6	6.3 ± 2.2	8.8 ± 0.5	9.3 ± 2.4	15.0 ± 3.4
3	1.9 ± 0.1	6.2 ± 1.3	6.8 ± 1.6	11.5 ± 1.2	11.0 ± 1.6	13.0 ± 2.3
4	2.9 ± 0.4	5.2 ± 1.5	11.0 ± 0.9	9.4 ± 0.5	12.4 ± 2.9	23.1 ± 3.0
5	11.7 ± 1.0	10.9 ± 1.0	14.8 ± 2.5	36.7 ± 5.5	31.3 ± 7.5	43.1 ± 5.3
	Time of flight (TF)			Full width half maximum (FWHM)		
Sample	20°C	25°C	30°C	20°C	25°C	30°C
1	8.0 ± 0.3	9.1 ± 1.0	13.9 ± 3.6	4.8 ± 1.3	5.8 ± 1.2	9.0 ± 3.8
2	9.8 ± 0.5	12.0 ± 2.5	20.5 ± 2.0	6.1 ± 2.2	9.2 ± 1.0	16.1 ± 1.5
3	15.0 ± 4.7	16.3 ± 1.8	21.5 ± 4.8	7.1 ± 1.0	11.0 ± 1.3	14.1 ± 1.8
4	11.2 ± 1.0	15.6 ± 2.8	25.5 ± 2.9	7.5 ± 0.4	9.4 ± 1.1	21.8 ± 2.3
5	37.3 ± 4.5	38.9 ± 1.8	37.5 ± 2.9	19.1 ± 1.8	26.0 ± 4.8	41.0 ± 6.1

[a]Values reported are average and SD of two independent runs.

TABLE 2
DSC Parameters for All Samples and All Crystallization Temperatures[a] (T_c)

	T_c = 20°C			T_c = 25°C			T_c = 30°C		
Samples	T_o (°C)	T_p (°C)	ΔH (J/g)	T_o (°C)	T_p (°C)	ΔH (J/g)	T_o (°C)	T_p (°C)	ΔH (J/g)
1	38.6	46.6	38.0	37.5	48.3	28.4	38.9	47.4	25.3
2	29.6	43.1	21.6	34.1	43.9	17.9	36.3	45.6	16.0
3	30.0	42.4	29.1	32.6	43.6	27.6	35.5	45.0	25.9
4	32.1	42.3	22.7	32.6	43.6	17.4	35.5	45.4	16.1
5	28.6	38.1	6.4	31.8	42.5	4.5	39.6	46.7	3.6

[a]T_o means onset temperature; T_p, peak temperature; and ΔH, enthalpy of melting.

Sample 4 could be crystallizing in a different polymorphic form at 30°C than at 25 and 20°C (16). The presence of small amounts of impurities could also induce nucleation, for example, in sample 3, resulting in a shorter induction time than expected.

Induction times calculated using ultrasonic parameters show the same tendency as the ones calculated with the laser turbidimeter technology. That is, for the same sample, induction times increased as crystallization temperature increased. When the crystallization behaviors of different samples were compared at a constant crystallization temperature, induction times increased as the m.p. of the sample decreased. One important difference is that although the tendencies are the same between methods, the induction time values obtained with the ultrasonic technology are significantly higher than the ones obtained with the laser. This means that IR, TF, and FWHM can be used to follow the crystallization process, but they should not be used to calculate induction times of nucleation since they lack sensitivity. Ultrasonic parameters change only when a visible amount of fat has already crystallized; thus, these parameters could be used to indicate induction times of bulk crystallization, but they are inappropriate to measure induction times of nucleation. The low sensitivity of this particular technique for determining induction times of nucleation can be explained by taking into account that ultrasonic waves are significantly affected by temperature fluctuations. Considering that phase transitions cause temperature changes, the accuracy of the ultrasonic velocity measurements can be affected by this local temperature variation especially at the beginning of the crystallization process.

Ultrasonic parameters changed on crystallization and, at some point, the ultrasonic signal started to attenuate as described by Martini *et al.* (5). This attenuation, however, did not depend on the induction times of crystallization of the samples. We expected shorter induction times to be associated with higher attenuations since more crystallized fat at a fixed time (90 min) was obtained. For example, when sample 2 was crystallized at 30°C the ultrasonic signal was completely attenuated, but when crystallized at 20 and 25°C (shorter induction time) only a partial attenuation was observed.

DSC. To study whether there was some correlation between the thermal behavior of the samples and the attenuation of the signal, DSC experiments were carried out on the five samples crystallized at the three temperatures assayed at the end of the experiment (90 min). Table 2 shows the DSC parameters (onset melting temperature, T_o; peak melting temperature, T_p; and melting enthalpy, ΔH) for all samples and crystallization temperatures. The thermal behavior of the samples did not have an effect on the attenuation of the ultrasonic signal since, although some differences were found in their thermal behavior, these were not correlated with the attenuation of the wave. For example, samples 2 and 4 show very similar thermal behavior at all crystallization temperatures, but sample 2 shows complete attenuation when crystallized at 30°C with the 550 kHz transducers, whereas sample 4 showed only small attenuation.

Fast Fourier transform (FFT) analysis. As crystallization takes place, SFC increases and some attenuation of the ultrasonic wave is observed; this attenuation can change with frequency. For samples crystallized at 20, 25, and 30°C, attenuation did not show any direct relationship with the SFC of the sample when using 550 kHz and 1 MHz transducers. This means that for the same SFC, some samples showed attenuation and some did not (5). To understand which factors affect the attenuation of an ultrasonic signal during crystallization of fats, an FFT spectrum was obtained from the SI. Figure 1 shows as an example the FFT spectrum with time of sample 3 crystallized at 30°C when measured with 1 MHz and 550 kHz transducers (a and b, respectively). The reader can see that when the sample temperature fell to the crystallization temperature, the magnitude of the FFT spectrum increased (approximately the first 5 min). Then it remained constant; and when crystallization started, the magnitude of the FFT spectrum decreased, showing some attenuation (65 min). Several peaks can be seen in the FFT spectra shown in Figures 1a and 1b, especially when the measurements were made with the 550 kHz transducers. This can be explained because this FFT data also contains the gain characteristics of the transducers (how the transducers respond at different frequencies) as well as the gain of the analog electronics and digital processing (different peaks on the plot), which make the analysis very complicated. These systematic gain corrections are not very interesting, and the first approach to minimize these peaks is to make a logarithmic plot of the magnitude as shown in Figures 1c and 1d. We can see that these plots are simpler and easier to analyze. Figures 1c and 1d also show how the ultrasonic wave is attenuated as crystallization takes place (for example, after 65 min of crystallization). A second approach to minimize the effect of the systematic gain corrections is to keep the chirp settings (frequency, duration, etc.) the same and record some of the images

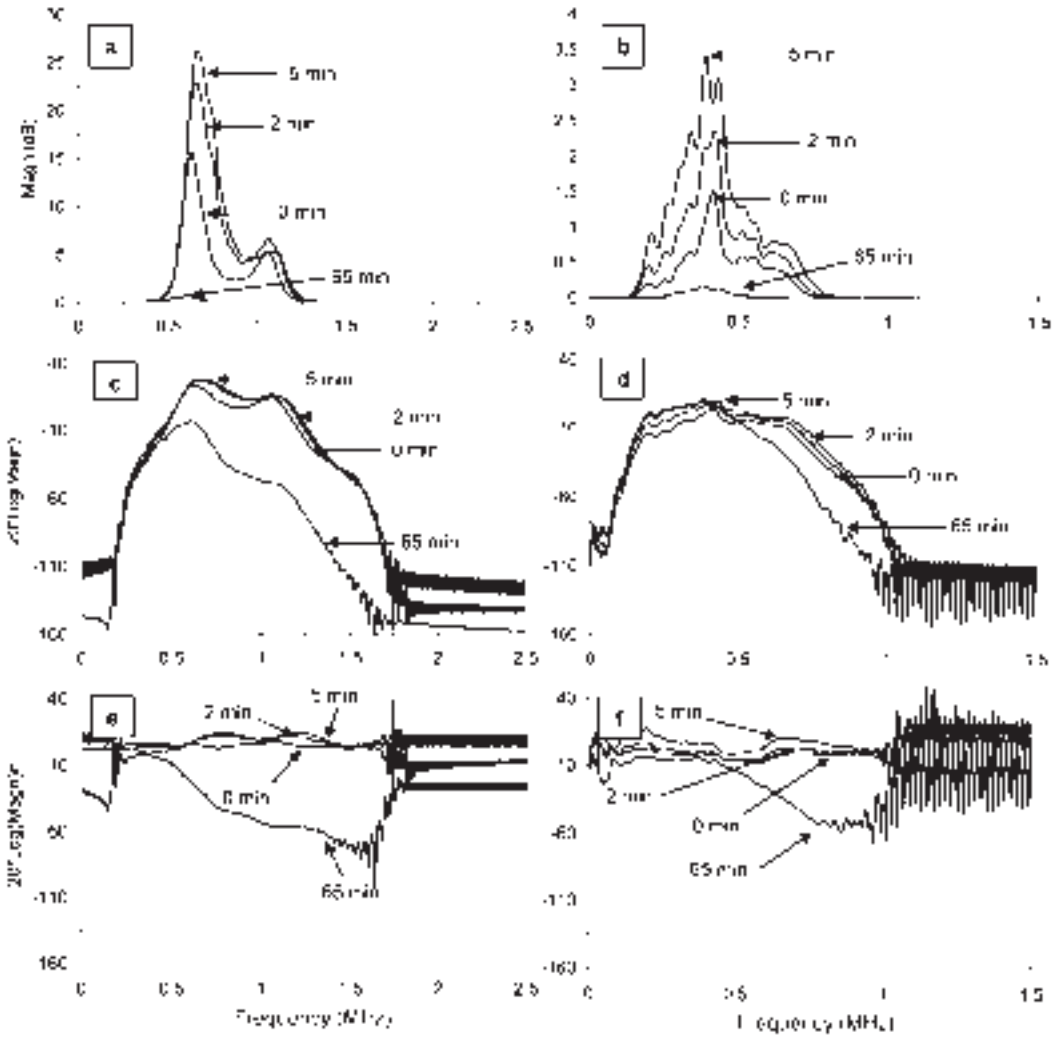

FIG. 1. Fast Fourier transform (FFT) plots of sample 3 crystallized at 30°C with 1 MHz (a) and 550 kHz (b) transducers. FFT log plot of sample 3 crystallized at 30°C with 1 MHz (c) and 550 kHz (d) transducers. Normalized FFT log plot of sample 3 crystallized at 30°C measured with 1 MHz (e) and 550 kHz (f) transducers. Effect of crystallization time (0, 2, 5, and 65 min) on FFT plots. Magn, magnitude of the signal; (Magn)n, normalized Magn.

through the cooling cell with canola oil (vegetable oil that does not crystallize under the experimental conditions used). These images are reference images that can be used to normalize away all the systematic effects that we do not want in our data. Therefore, the canola oil images (log plots) were subtracted from the sample ones (log plots). Figures 1e and 1f show as an example the normalized FFT data of sample 3 crystallized at 30°C measured with the 1 MHz and 550 kHz transducers, respectively. This figure shows the variation in the magnitude of the ultrasonic signal (expressed in the logarithmic form) with frequency during the crystallization process. We can see that the attenuation starts at high frequencies and, as the crystallization process continues, lower frequencies are attenuated. It can also be seen that 1 MHz transducers showed more attenuation (for the same crystallization time) than the 550 kHz transducers. The same general behavior shown in Figure 1 was observed for all samples at all crystallization temperatures assayed and with both transducers.

To quantify the attenuation of each sample, we plotted the magnitude of the normalized log signal at 550 kHz and 1 MHz against time for all samples and all crystallization temperatures assayed (Fig. 2). Canola oil data were also reported here to compare the behavior of the samples with a sample that did not show any crystallization at the temperatures chosen. It is important here to differentiate different kinds of attenuation. The ultrasonic signal can be slightly attenuated, especially at the beginning of the crystallization process but, in this case, the second transducer can still detect a signal after passing through the sample (Fig. 2a, sample 1). In this case, high frequencies are being scattered from the ultrasonic wave as shown by the FFT plots, and the change in the magnitude of the ultrasonic signal is between 0 and 50 dB approximately. On the other hand, some samples completely attenuate the ultrasonic signal; and therefore the transducer is not able to detect any signal after passing through the sample (Fig. 2c, sample 3), i.e., both high and low frequencies are being completely attenuated. In these

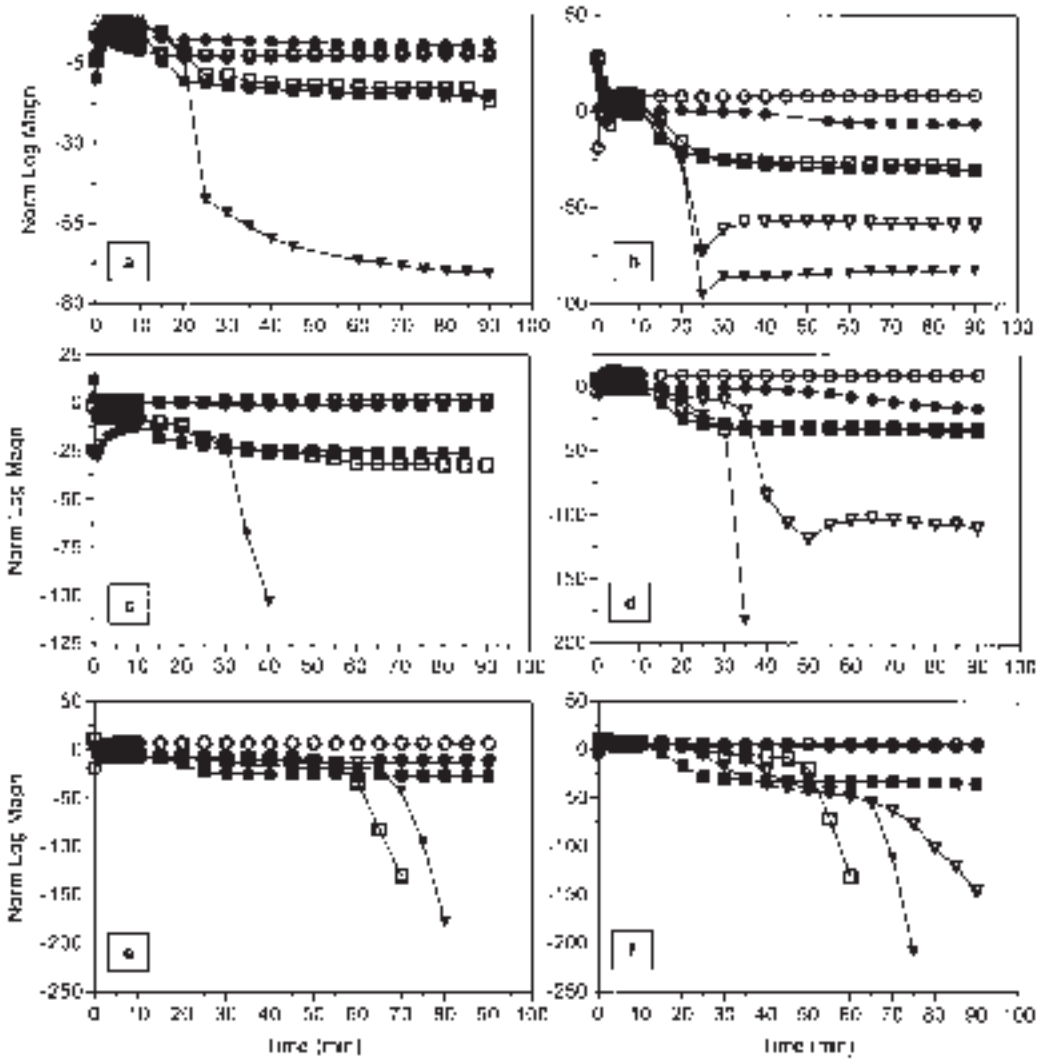

FIG. 2. Normalized log plots of all samples crystallized at 20°C with the 550 kHz (a) and 1 MHz (b) transducers; at 25°C with the 550 kHz (c) and 1 MHz (d) transducers; and at 30°C with the 550 kHz (e) and 1 MHz (f) transducers. ■, □, ▼, ▽, ●, and ○ for samples 1, 2, 3, 4, 5, and canola oil, respectively.

cases, the ultrasonic wave magnitude changes ~100 dB. Samples can also attenuate the ultrasonic signal at some point in between these two extremes. In these cases, the signal can still be detected by the second transducer but the attenuation is very high, as for example sample 3 crystallized at 20°C (Fig. 2a). Now, the variation of ultrasonic signal magnitude is between 50 and 100 dB. This kind of attenuation usually starts when the sample reaches a constant SFC value. This means that although the SFC is stabilizing, the ultrasonic parameters continue to vary (the attenuation continues). This indicates that signal attenuation may depend on the SFC, especially during the first part of the crystallization process, but there may be some other factors that influence the decrease of the ultrasonic signal when SFC is constant.

From Figure 2 we can also see that data obtained with 1 MHz transducers seemed to be more sensitive since, in some cases, attenuation was observed at shorter times when compared with the 550 kHz transducer data. Sample 4 crystallized at 20, 25, and 30°C did not show attenuation when the measurements were performed with the 550 kHz transducers but did show some kind of attenuation when measured with the 1 MHz transducers. In general, a high or complete attenuation occurred earlier when the ultrasonic parameters were measured using 1 MHz transducers (for example, sample 3 crystallized at 25 and 30°C and sample 2 crystallized at 30°C).

Microstructure. As mentioned in the introduction, several factors can cause the attenuation of an ultrasonic wave. One of these factors is the absorption of ultrasound owing to thermodynamic relaxation mechanisms such as phase transitions. The other factor that causes attenuation is scattering from the particles themselves and from the presence of interfaces. It is very difficult to separate these phenomena in a crystallization process, but they are all directly related to the size and structure of the crystals and aggregates in the system. Therefore, to inter-

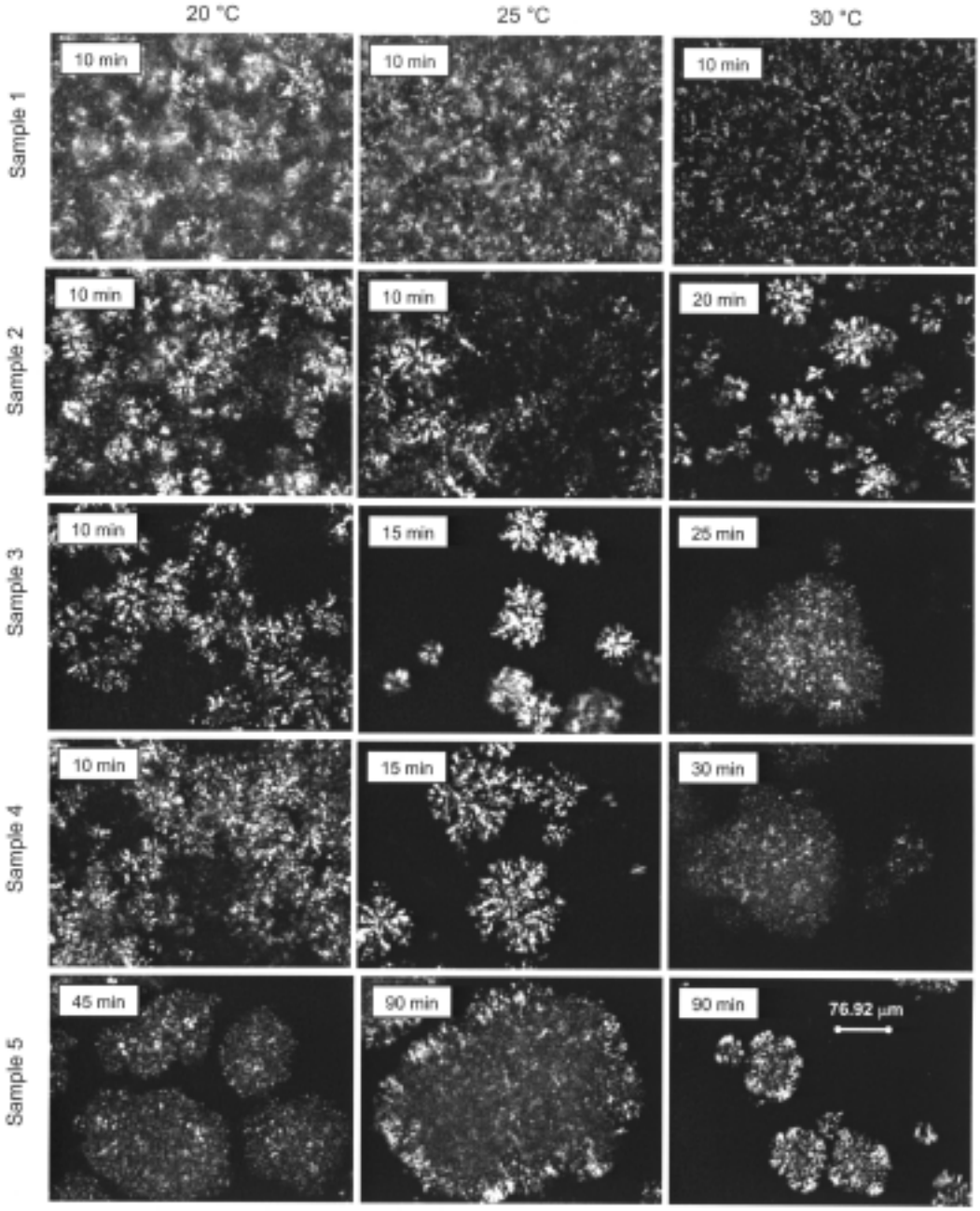

FIG. 3. Polarized light micrographs of fat samples crystallized at 20, 25, and 30°C with solid fat content (SFC) of approximately 5%.

pret the variation of the magnitude of the ultrasonic signal shown in the FFT data (attenuation), we analyzed the microstructure of the samples as crystallization took place. Samples showed slightly different morphologies. Sample 1 had needle-shaped crystals when crystallized at all temperatures, especially at early times of the crystallization process. As crystallization time increased, these needles organized themselves to form clusters of crystals. The same behavior was observed for sample 2 crystallized at 20 and 25°C. For the other conditions, none of the crystals obtained were single crystals but rather were clusters of needles. As crystallization temperature decreased and crystallization time increased, these clusters became more densely packed, and a well-defined spherical shape was observed. Although the morphology was almost the same for all the crystallization conditions assayed, the crystal size was significantly different, especially for samples that were only slightly supercooled. Differences in crystal size were more evident at higher temperatures (25 and 30°C) and in general, low degrees of supercooling resulted in bigger crystals. Micrographs of crystals with the same SFC value were chosen to compare their morphologies and study how these factors affected the attenuation of the ultrasonic signal (Figs. 3–6). Comparing

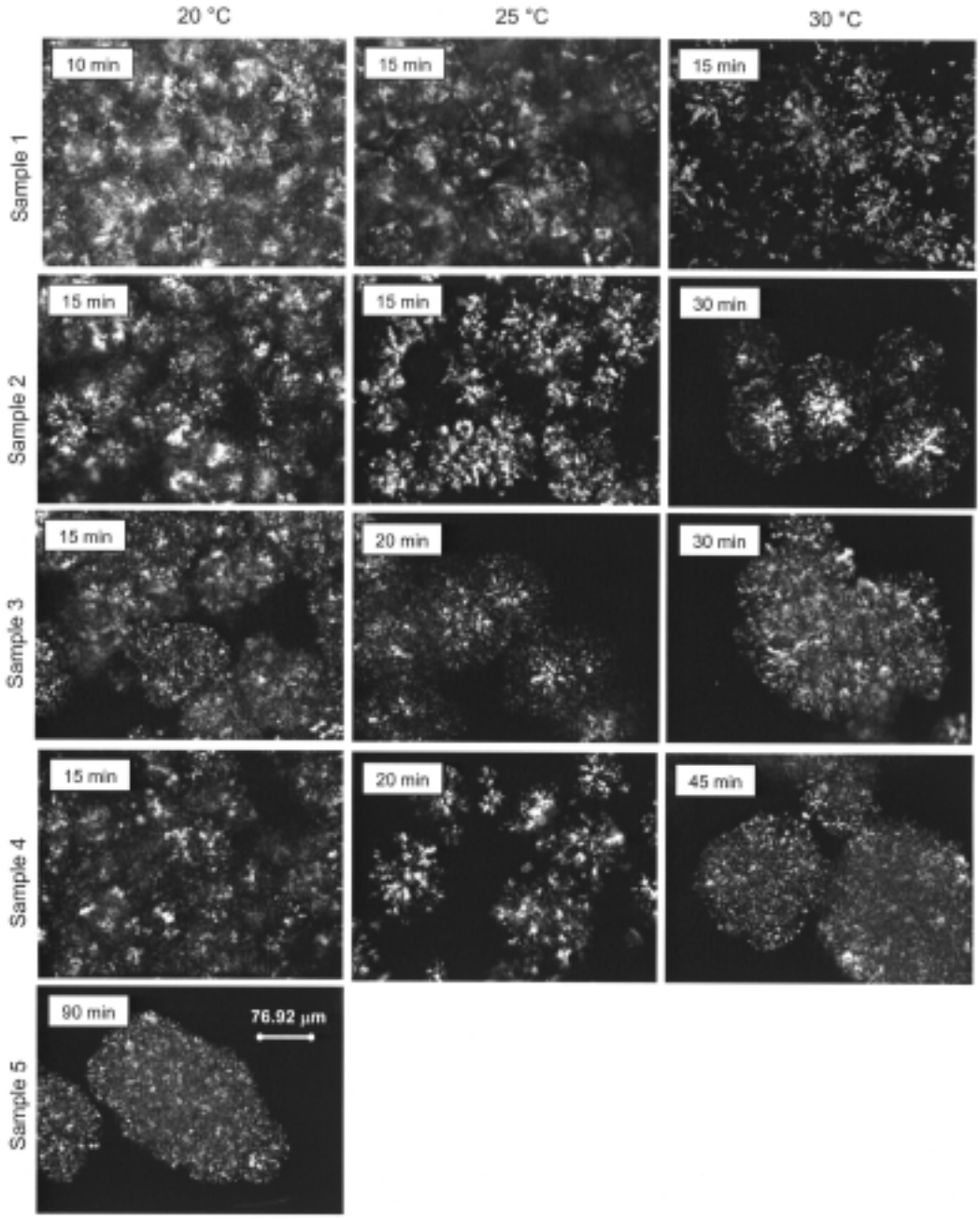

FIG. 4. Polarized light micrographs of fat samples crystallized at 20, 25, and 30°C with SFC of approximately 10%. For abbreviation see Figure 3.

these figures with Figure 2 and the FFT data, we can ascertain how the microstructure and SFC affected the attenuation. Figure 3 shows micrographs of all samples crystallized at 20, 25, and 30°C with an SFC of ~5%. Samples 3 and 4 crystallized at 30°C showed low attenuation. The same behavior was observed in sample 5 crystallized at 25°C (data obtained from the FFT plots). These samples reached 5% SFC after 25, 30, and 90 min of crystallization, respectively. Comparing the crystals in these samples with the ones that did not show attenuation at all, we can see that crystal size might be affecting the attenuation of the ultrasonic signal since samples that showed attenuation have significantly larger crystals than the ones that did not show attenuation at a constant SFC value (5%).

Figure 4 shows micrographs of the same samples crystallized at the crystallization temperatures assayed but at a time when they had reached approximately 10% of solid fat. All the samples shown here exhibited a slight attenuation of the ultrasonic wave (between 0 and 50 dB of variation) independent of the crystal sizes. Even for small crystals, as shown in sample 1, crystallized at 20, 25, and 30°C, there is some attenuation of the signal due to the increase in the SFC value.

Figure 5 shows crystals of samples with 15% SFC. As

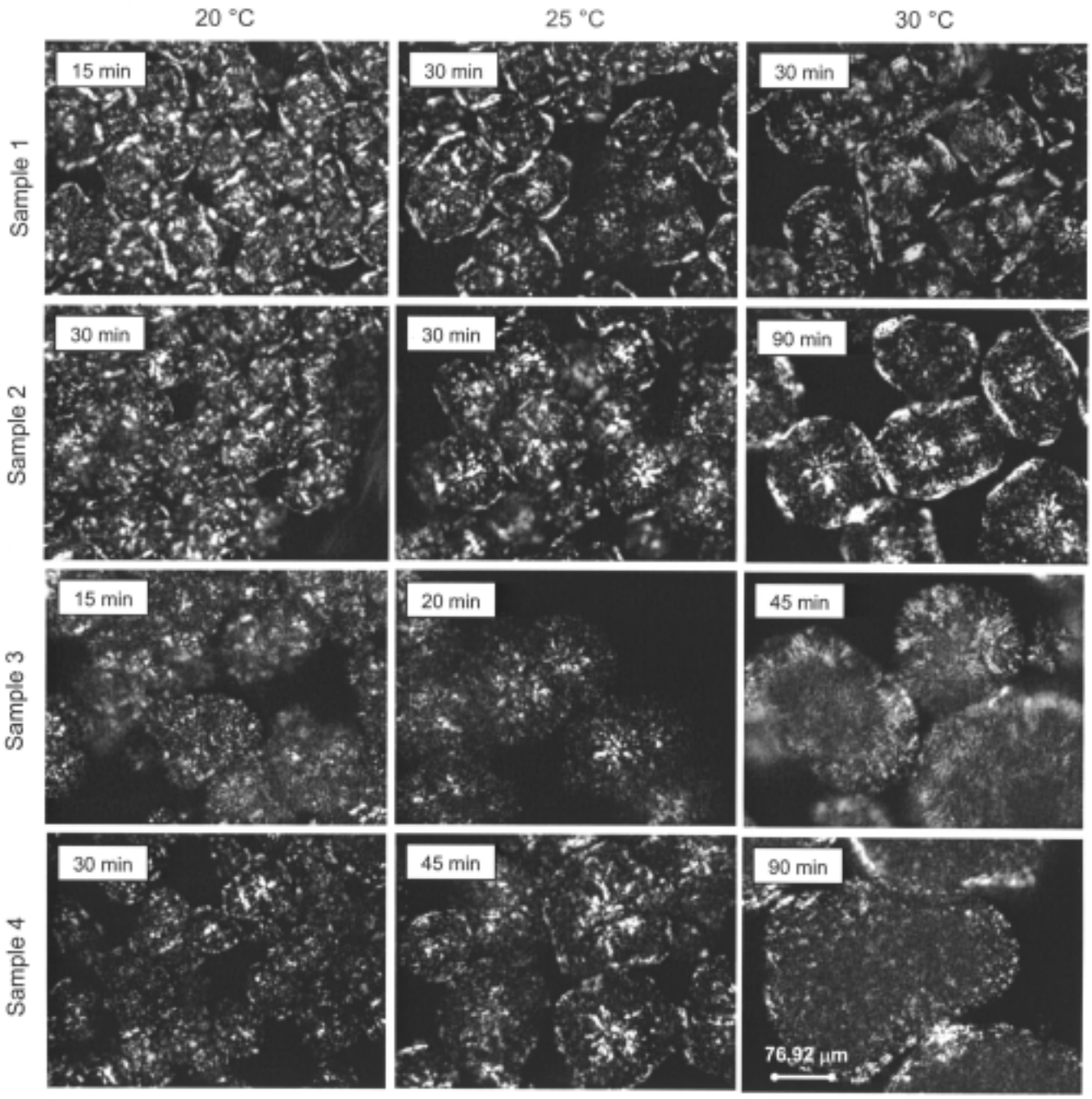

FIG. 5. Polarized light micrographs of fat samples crystallized at 20, 25, and 30°C with SFC of approximately 15%. For abbreviation see Figure 3.

shown in Figure 4, all crystals caused at least a slight attenuation. But sample 2, crystallized at 30°C, and sample 4, crystallized at 25 and 30°C, showed total attenuation of the ultrasonic signal (variation of more than 100 dB) due to the larger size of their crystals (compare Figs. 5 and 2). A good example of how crystal size results in a complete attenuation of the ultrasonic signal can be seen by comparing pictures of sample 2 crystallized at 20, 25, and 30°C with SFC of approximately 15% (Fig. 5), where higher crystallization temperatures generate larger crystals and therefore a total attenuation is observed.

Although sample 3 crystallized at 30°C showed larger crystals than sample 2 crystallized at the same temperature (Fig. 5), it did not show complete attenuation of the ultrasonic signal when it reached ~15% SFC (45 min), as shown in Figure 2. This fact suggests that there might be some other factors that affect the attenuation of the signal. One possibility is how the fat crystals are packed to form the cluster. For example, sample 2 crystal clusters have more defined edges, and although the SFC of both samples 2 and 3 are not significantly different (14.0 and 14.3% for samples 2 and 3, respectively), the crys-

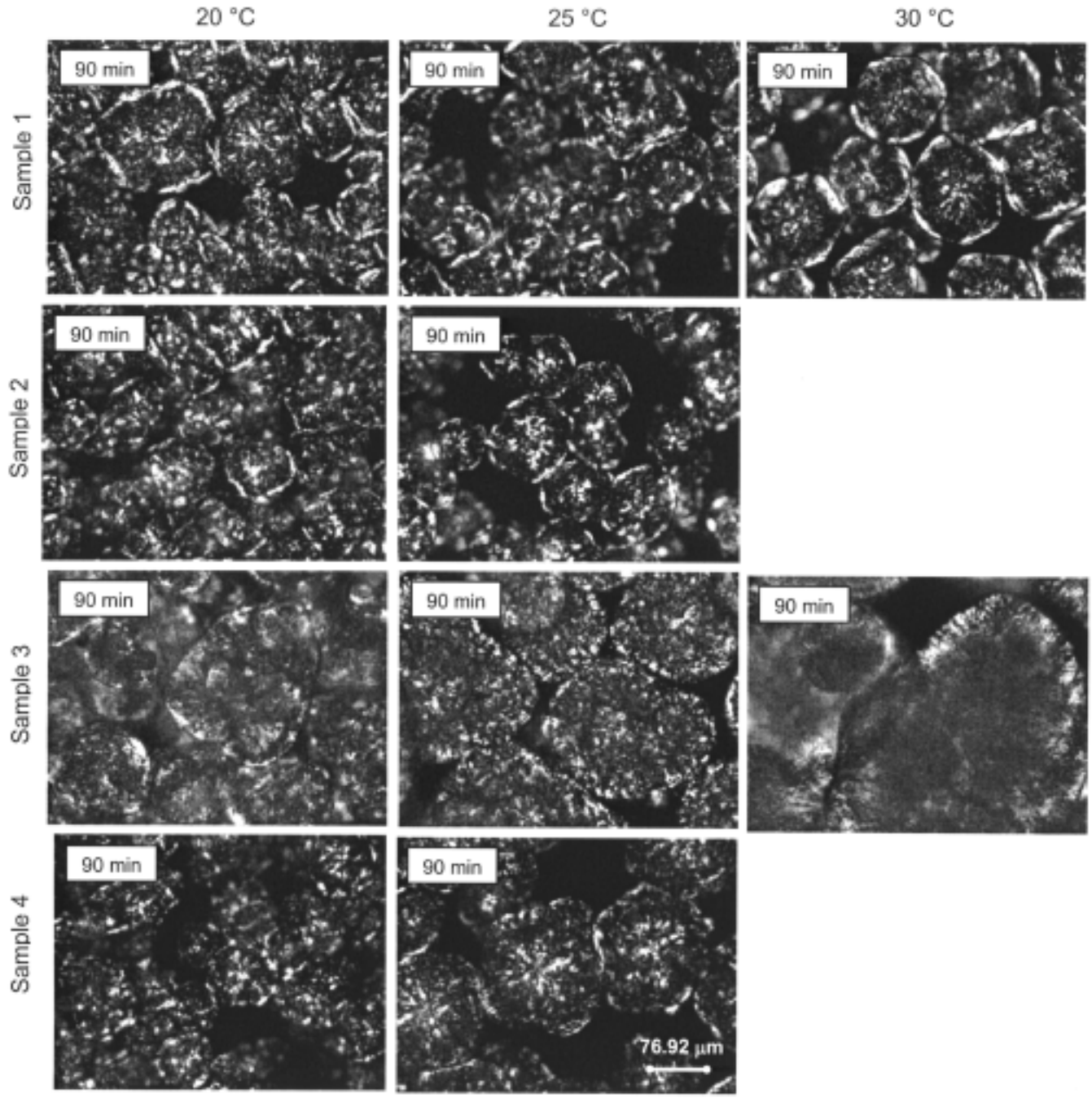

FIG. 6. Polarized light micrographs of fat samples crystallized at 20, 25, and 30°C with SFC of approximately 20%. For abbreviation see Figure 3.

tals in sample 2 seemed to be more densely packed than in sample 3.

Figure 6 includes pictures of the samples when they reached a higher SFC (approximately 20%). Sample 3 crystallized at 20, 25, and 30°C shows complete attenuation together with sample 4 crystallized at 25°C. These samples contain very large crystals, which are responsible for the complete attenuation of the signal. Comparing these data with the data analyzed in Figure 5, we can see that sample 3 requires around 20% of solids so as to attenuate the ultrasonic signal. We note in this figure that even though sample 1 crystallized at 20, 25, and 30°C has a very high SFC (20.1, 20.1, and 17.4%, respectively) it displays a high, but not complete, attenuation of the signal. This can be explained because the crystals are not large enough to scatter the ultrasonic wave completely.

At low SFC, crystal size seems to affect the attenuation of ultrasonic waves. As SFC increases, especially at intermediate SFC values, the signal is attenuated even though crystals are small. In this range therefore, the SFC is mainly responsible for signal attenuation. At higher SFC values, crystal size seems to be responsible for the complete attenuation of the signal (sample 4 crystallized at 25 and 20°C in Figure 6 has SFC val-

ues of 15.7 and 17.1%, respectively, and the first one, which has larger crystals, shows complete attenuation). However, even when the SFC is high, complete attenuation is not guaranteed, as shown by sample 1 with an SFC of 20%.

In summary, ultrasonic technology can be used to monitor the crystallization process of fats. Ultrasonic parameters are useful tools to monitor the bulk crystallization of these systems and can be used to determine SFC of the crystallized fat. Although the technology developed in this study uses a signal that can go through a large amount of crystallized fat, the system usually attenuates at ~20% SFC. The attenuation observed did not depend on the induction times of crystallization, or on the thermal behavior of the crystals, but it did depend on SFC and microstructure, especially on the crystal size. Attenuation occurs first at higher frequencies. The factors that influence signal attenuation are strongly correlated. For low SFC (5%), attenuation is due to crystal size, but when SFC increases to intermediate levels (10%), crystal size seems not to be very important since attenuation is observed even for small crystals. When SFC is higher (up to 20%), crystal size seems to be the factor that controls attenuation again.

ACKNOWLEDGMENTS

The authors acknowledge the financial support of the Natural Sciences & Engineering Research Council of Canada (NSERC) and the Ontario Ministry of Food (OMAF). Dr. Martini thanks the National Research Council of Argentina (CONICET) for her postdoctoral fellowship. We also thank Dr. Gianfranco Mazzanti for technical assistance.

REFERENCES

1. McClements, D.J., Ultrasonic Characterization of Emulsions and Suspensions, *Adv. Colloid Interface Sci. 37*:33–72 (1991).
2. McClements, D.J., and M.J.W. Povey, Ultrasonic Analysis of Edible Fats and Oils, *Ultrasonics 30*:383–388 (1992).
3. McClements, D.J., M.J.W. Povey, and E. Dickinson, Absorption and Velocity Dispersion Due to Crystallization and Melting of Emulsion Droplets, *Ibid. 31*:433–437 (1993).
4. McClements, D.J., and P. Fairley, Frequency Scanning Ultrasonic Pulse Echo Reflectometer, *Ibid. 30*:403–405 (1992).
5. Martini, S., C. Bertoli, M.L. Herrera, I. Neeson, and A.G. Marangoni, *In situ* Monitoring of Solid Fat Content by Means of Pulsed Nuclear Magnetic Resonance Spectroscopy and Ultrasonics, *J. Am. Oil Chem. Soc. 82*, 305–312 (2005).
6. Saggin, R., and J.N. Coupland, Shear and Longitudinal Ultrasonic Measurements of Solid Fat Dispersions, *Ibid. 81*:27–32 (2004).
7. Saggin, R., and J.N. Coupland, Rheology of Xanthan/Sucrose Mixtures at Ultrasonic Frequencies, *J. Food Eng. 65*:49–53 (2002).
8. Sigfusson, H., G.R. Ziegler, and J.N. Coupland, Ultrasonic Monitoring of Food Freezing, *Ibid. 62*:263–269 (2004).
9. Bamberger, J.A., and M.S. Greenwood, Using Ultrasonic Attenuation to Monitor Slurry Mixing in Real Time, *Ultrasonics 42*:145–148 (2004).
10. Miles, C.A., G.A.J. Fursey, and R.C.D. Jones, Ultrasonic Estimation of Solid/Liquid Ratios in Fats, Oils and Adipose Tissue, *J. Sci. Food Agric. 36*:215–228 (1985).
11. McClements, D.J., and M.J.W. Povey, Comparison of Pulsed NMR and Ultrasonic Velocity Techniques for Determining Solid Fat Contents, *Int. J. Food Sci. Technol. 23*:159–170 (1988).
12. McClements, D.J., and M.J.W. Povey, Investigation of Phase Transitions in Glyceride/Paraffin Oil Mixtures Using Ultrasonics Velocity Measurement, *J. Am. Oil Chem. Soc. 65*:1791–1795 (1988).
13. Singh, A.P., D.J. McClements, and A.G. Marangoni, Comparison of Ultrasonic and Pulsed NMR Techniques for Determination of Solid Fat Content, *Ibid. 79*:431–437 (2002).
14. Saggin, R., and J.N. Coupland, Measurement of Solid Fat Content by Ultrasonic Reflectance in Model Systems and Chocolate, *Food Res. Intl. 35*:999–1005 (2002).
15. Singh, A.P., D.J. McClements, and A.G. Marangoni, Solid Fat Content Determination by Ultrasonic Velocimetry, *Ibid. 37*:545–555 (2004).
16. Herrera, M.L., C. Falabella, M. Melgarejo, and M.C. Anon, Isothermal Crystallization of Hydrogenated Sunflower Oil: I-Nucleation, *J. Am. Oil Chem. Soc. 75*:1273–1280 (1998).

[Received September 30, 2004; accepted April 19, 2005]